PHYSICAL REVIEW A VOLUME 57, NUMBER 2 FEBRUARY 1998

Microscopic lens effect in photoelectron imaging spectroscopy

C. Bordas and J. C. Pinaré
Laboratoire de Spectrométrie Ionique et Moléculaire, UMR CNRS 5579, Université Claude Bernard Lyon 1, Bâtiment 205, 43 Boulevard du 11 Novembre 1918, F69622 Villeurbanne Cedex, France

(Received 30 July 1997)

The photoelectron imaging spectrometer has been used to investigate the resonant multiphoton ionization of xenon and hydrogen. Under certain conditions, extremely sharp unexpected features appear in the photoelectron images. It is shown that these features are produced by the residual ions acting as a microscopic lens that distorts the trajectories of the photoelectrons. The relevance of this phenomenon in zero electron kinetic energy spectroscopy and in experiments concerned with angular distribution measurements in strong-laser-field multiphoton ionization or in the photodetachment microscope is discussed.
[S1050-2947(98)50202-8]

PACS number(s): 33.60.−q, 33.80.Rv

Experimental and theoretical studies of the Stark effect [1,2] in hydrogenic systems have been initiated in the early days of quantum mechanics. The understanding of the structure and dynamics of a simple quantum system in an external electric field is indeed a fundamental problem relevant to various physical processes such as photoionization or Rydberg states spectroscopy [3]. It is well known that the specific shape of this potential, which presents a saddle point located at energy $-\sqrt{2F}$, is responsible for the so-called field-induced ionization. The study of field-induced [4–6] or forced [7,8] ionization has been the subject of many articles and is directly at the origin of zero electron kinetic energy (ZEKE) spectroscopy [9–12]. In a series of famous papers, Fabrikant [13] and Kondratovitch and Ostrovsky [14] have discussed the classical motion of electrons in a hydrogenic system in a static external field and have developed a semiclassical analysis able to describe the interference patterns resulting from the different paths followed by the electrons. These papers are directly at the origin of the photodetachment microscope described recently by Blondel *et al.* [15]. The principle of the photoelectron imaging spectrometer developed by Helm and co-workers [16] and used in the present work is also more or less contained in these papers. Our experimental results obtained in a photoelectron imaging spectrometer show that one cannot neglect the interaction of ejected electrons with the residual ions, even in conditions where their energy is, *a priori*, large enough to do so.

The photoelectron imaging spectrometer used in the present experiments has been described in detail previously [16,17] as well as the numerical procedures [18] used to extract the meaningful information from the raw experimental data. Briefly the operation of the imaging spectrometer is as follows: when electrons are ejected with a given kinetic energy W in the focal region of the laser at time $t=0$, they are later found on the surface of a sphere expanding linearly with time. An external homogeneous field is applied to project this sphere onto a position-sensitive detector (multichannel plates and phosphor screen). This results in the observation of a circular image of electron impacts with a diameter proportional to $\sqrt{W}$ and a filling pattern that reveals the spatial distribution of the electrons and their initial angular distribution. If the polarization of the laser is set perpendicular to the electric field (i.e., parallel to the plane detector), the image contains all the information relative to the initial energetic and angular distributions. The screen image is monitored with a charge-coupled-device (CCD) camera and accumulated in a microcomputer. A statistically meaningful image is obtained by the digital summing of electron impacts from several thousands of laser shots. Figure 1 presents a schematic view of the apparatus. In the experiments described here [17], the vacuum chamber is filled with xenon, a tunable pulsed dye laser (20 ns, $\leqslant$1.0 mJ/pulse) is focused on a diameter of about 15 μm at the center of the spectrometer, and the applied field is $F=22.7$ V/cm. A typical experimental image recorded with $P_{\mathrm{Xe}}=2\times10^{-6}$ Torr is presented in Fig. 2(a). The laser is tuned in resonance with a three-photon ($\lambda=357.61$-nm) transition toward the

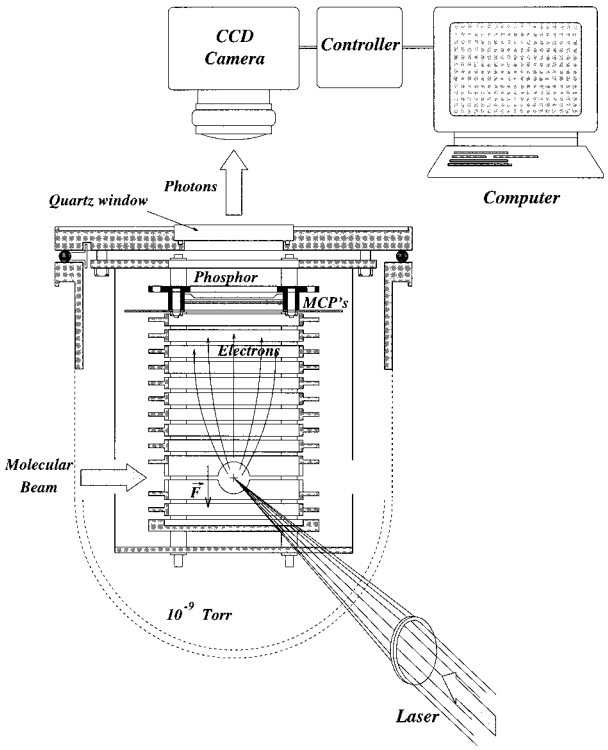

FIG. 1. Schematic view of the experimental setup.

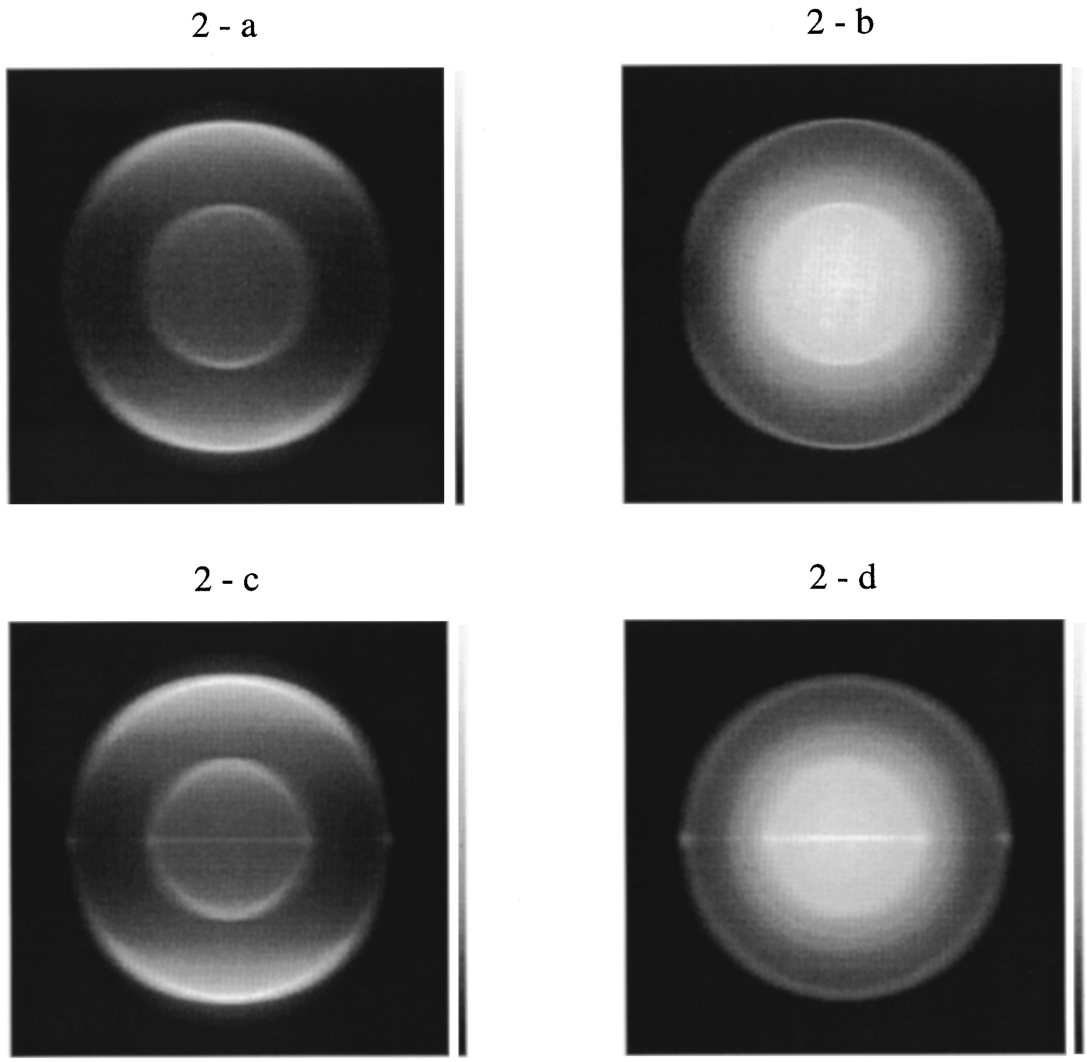

FIG. 2. Images obtained in $(3+1)$ photon ionization of xenon with the $5d[3/2]J=1$ intermediate state and a field $F=22.7$ V/cm. (a) Polarization perpendicular to the electric field, $P_{Xe}=2.10^{-6}$ Torr, $500e^-$/ laser shot; (b) polarization parallel to the field, $P_{Xe}=2.10^{-6}$ Torr; $500e^-$/shot; (c) polarization perpendicular to the field, $P_{Xe}=2.10^{-5}$ Torr; $5000e^-$/shot; (d) polarization parallel to the field, $P_{Xe}=2.10^{-5}$ Torr; $5000e^-$/shot. In (a) and (c), the laser polarization is vertical in the plane of the image, while it points towards the observer in (b) and (d). The gray scale (on the right of each image) ranges from 0% (black) to 100% (white) of the relative maximum electron signal. The distance between the ionization region and the detector is $L=88$ mm and the size of the square image is 44 mm.

$5d[3/2](J=1)$ state. The absorption of a fourth photon brings the system above the two final ion channels $Xe^+\ ^2P_{3/2}$ (ground state) and $Xe^+\ ^2P_{1/2}$ (excited state). The electrons formed in the ground- and excited-state channels are ejected with an initial kinetic energy of 1.74 and 0.43 eV, respectively. Two concentric circular rings appear on the image: the outer ring corresponds to electrons leaving the core in its ground state, the inner ring to those leaving the core in its excited state. Figure 2(a) is recorded with the laser polarization perpendicular to the electric field. Under these conditions, the angular distribution of the photoelectrons may be extracted from the experimental image [18]. Figure 2(b) has been recorded under the same experimental conditions, except that the light is polarized parallel to the field. As a consequence, the image is isotropic and the information relative to the angular distribution is lost. If, by any experimental means, such as increasing of the laser fluence or gas density, one increases the photoelectron signal, a very specific phenomenon appears: namely, the observation of a thin equatorial line in the experimental images. This thin line, indicating a very sharp electron emission limited to a direction perpendicular to the light polarization, has been observed for all intense transitions in $(3+1)$-photon ionization of xenon and also in H_2 [19]. This seemingly general effect is clearly visible in Fig. 2(c), which has been recorded under the same experimental conditions as the image of Fig. 2(a), except that $P_{Xe}=2\times10^{-5}$ Torr. As a consequence, the number of electrons ejected per laser shots is about ten times larger. This effect being observed either by increasing the laser intensity or the gas density, at least three different processes can be suspected to produce it: (i) a light intensity effect directly affecting the angular distribution by modifying the radiative field-atom coupling and inducing a sharp peak at 90° in the angular distribution; (ii) a modification of the electron escape trajectory due to a ponderomotive effect; and (iii) a ''pure'' space-charge effect. Actually, processes (i) and (ii) may be ruled out simply by comparison of Figs. 2(a) and 2(c). The laser characteristics (intensity, duration, focusing) are quite

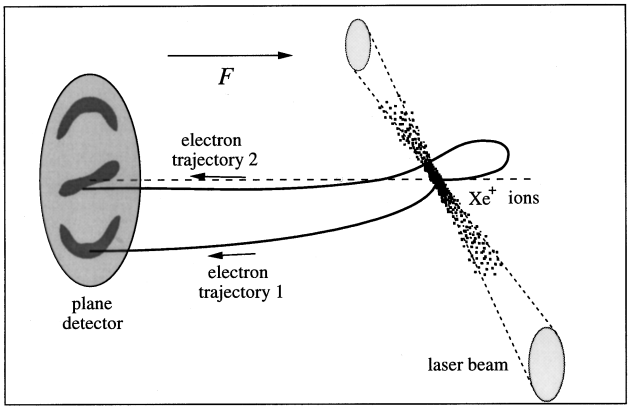

FIG. 3. Schematic of the microscopic lens effect. The trajectory of an electron emitted toward the detector (trajectory 1) is not perturbed by the charge distribution, while an electron emitted in the opposite direction (trajectory 2) may be deflected by the residual ions.

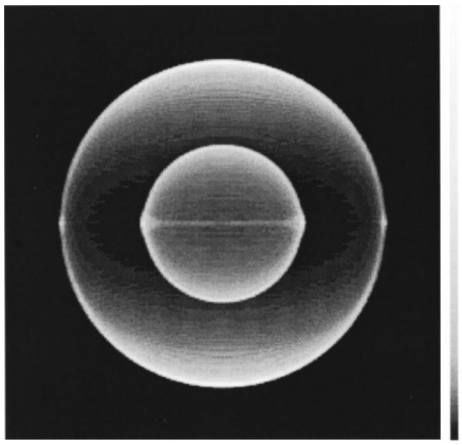

FIG. 4. Numerical simulation of the image of Fig. 2(c) computed with the angular distributions derived from the image of Fig. 2(a) and a charge distribution characterized by $N_e = 5000$, $L = 500\ \mu$m. Same scale as in Fig. 2.

similar in both images, and since the gas density is increased by a factor of 10 in image (c), only a process linked to the higher number of positive and negative charges created in the ionization process is likely. Moreover, the image of Fig. 2(d) recorded in the same experimental conditions as image 2(c), except for the laser polarization, which is set parallel to the field, shows that the appearance of the sharp equatorial line is not governed by the laser polarization. In the images of Figs. 2(a) and 2(b), we can estimate the number of electrons ejected to about 500 per laser shot. On the other hand, images of Figs. 2(c) and 2(d) where the equatorial line is visible have been obtained with about 5000 electrons per laser shot. Hence, both series of images have been obtained with, respectively, 500 and 5000 residual ions in the interaction region where ionization occurs. This region, defined by the focusing geometry of the laser is roughly 0.5 mm long and 15 μm in diameter. The residual positive charges are almost at rest with respect to the electrons and therefore create a large attractive potential. Due to the elongated shape of the ionization region and hence of the charge distribution, which creates this attractive potential, the effective potential behaves roughly like a microscopic cylindrical lens. The trajectory of the electrons emitted towards the detector is hardly perturbed by this microscopic lens. On the other hand, electrons emitted in the opposite direction will again pass close to the residual ions and those emitted in the vicinity of the plane defined by the electric field and the propagation direction of the laser (major axis of the lens) will be deflected. This qualitative explanation is schematized in Fig. 3. This deflection creates on the final image, whatever the polarization, a sharp electron distribution parallel to the laser propagation. A simple classical numerical simulation has been undertaken in order to justify this hypothesis. At first order, the attractive potential generated by the N residual ions may be approximated by the potential generated by a wire of length L (effective length of the charge distribution, close to twice the Rayleigh length), uniformly charged (total charge Nq). Strictly speaking, N increases from 0 to its final maximum value during the 20-ns laser pulse. This can be accounted for phenomenologically in the simulation by choosing an average N value. Assuming this attractive potential and the energetic and angular photoelectron distribution derived from reliable low-density experiments, a qualitative agreement between experiment and simulation may be obtained that confirms the relevance of our hypothesis. The simulated image presented in Fig. 4 has been computed with the measured distributions combined with the following parameters: $N = 5000$; $L = 500\ \mu$m.

Beyond the somewhat anecdotal aspect of this effect, this observation is indeed of general interest and relevant to many experimental situations involving photoionization, all the more so when one is concerned with low-energy electrons. The experimental results presented here show that (i) sharp features observed in photoelectron angular distributions must be analyzed with great care and (ii) electrons ejected with an energy on the order of 1 eV are sensitive to the presence of a few thousand positive charges. Concerning the first point, several examples of published angular distributions show a sharp intensity-dependent peak at 90° with respect to polarization. Without casting any doubts on these measurements, the images presented in Fig. 2 show that one can easily be mistaken about the origin of sharp peaks of photoelectrons emitted at 90°. As far as point (ii) is concerned, the microscopic optics resulting from the presence of ions in the interaction volume may have interesting applications or consequences. Indeed, fast electrons (typically 1 eV) are nevertheless extremely sensitive to a microscopic lens made of a few thousand ions. From a topological point of view [14,20], electron trajectories obey a scaling law where the key quantity is the ratio W/F between the kinetic energy of the electron and the total electric field (Coulomb plus Stark). That is to say, effects of the same order of magnitude could be expected for electrons in the meV range interacting with only a few positive charges. This inference has obvious consequences in the whole field of ZEKE spectroscopy [9–12], where one is concerned with electrons of 0.01–0.1 meV in external fields of about 1 V/cm interacting with a possibly large number of ions. It is easy to understand how slow electrons may be trapped in the potential well of residual ions, at least as long as these ions are confined in a volume small enough to generate an attractive potential larger than the asymptotic kinetic energy. This aspect could partly ex-

plain the anomalously long lifetime of ZEKE states [21–23] and particularly the lengthening of that lifetime when the number of electrons increases, which has been previously explained by the loss of axial symmetry (and subsequently of m_l) in the presence of distributed charges. For example, if one considers the interaction of a slow electron ejected with a kinetic energy on the order of 1 meV in a field of a few V/cm interacting with the single ion from which it has been removed, an exact classical trajectory calculation [14,20] shows that the image splits into two rings with an inner ring corresponding to electrons emitted towards the detector and an outer ring corresponding to electrons of the same energy emitted in the opposite direction. This behavior, which is the single particle analogous to the present microscopic lens effect, will be discussed in detail in a separate paper. Under these conditions, it appears that the asymptotic electron-ion interaction must be taken into account on dimensions of the order of several μm as soon as one is concerned with electrons having a kinetic energy of a fraction of meV ($\approx 1\ \mathrm{cm}^{-1}$). It is almost certain that such interactions produce unexpected effects, not only in ZEKE experiments [9–12,21–23], but also in an experiment such as the photodetachment microscope developed by Blondel *et al.* [15], which is based on the same principle as the imaging spectrometer.

As a conclusion, let us finally mention that the observation of the analog of the microscopic lens effect for a single electron-ion system could probe the very long-range interaction (μm scale) between the electron and the ionic core and that our observation gives an indication of the possibility of achieving electron optics at the microscopic scale.

Fruitful discussions with H. Helm and M. Broyer and the technical support of M. Barbaire, J. Maurelli, and F. Valadier are gratefully acknowledged. The Laboratoire de Spectrométrie Ionique et Moléculaire is ''Unité Mixte de Recherche'' CNRS–Université Lyon I, No. 5579.

[1] See, for example, H. A. Bethe and E. E. Salpeter, *Quantum Mechanics of One- and Two-Electron Atoms* (Plenum, New York, 1977).
[2] D. A. Harmin, Comments At. Mol. Phys. **15**, 281 (1985).
[3] T. F. Gallagher, *Rydberg Atoms* (Cambridge University Press, Cambridge, England, 1994); R. F. Stebbings and F. B. Dunning, *Rydberg States of Atoms and Molecules* (Cambridge University Press, Cambridge, England, 1983).
[4] J. E. Bayfield and P. M. Koch, Phys. Rev. Lett. **33**, 258 (1974).
[5] P. M. Koch and D. R. Mariani, Phys. Rev. Lett. **46**, 1275 (1981).
[6] C. Bordas, P. Brevet, M. Broyer, J. Chevaleyre, and P. Labastie, Europhys. Lett. **3**, 789 (1987).
[7] W. R. S. Garton, W. H. Parkinson, and E. M. Reeves, Proc. R. Soc. London, Ser. A **80**, 860 (1962).
[8] W. Sandner, K. A. Safinya, and T. F. Gallagher, Phys. Rev. A **33**, 1017 (1986).
[9] K. Müller-Dethlefs, M. Sander, and E. W. Schlag, Chem. Phys. Lett. **112**, 291 (1984).
[10] K. Müller-Dethlefs and E. W. Schlag, Annu. Rev. Phys. Chem. **42**, 109 (1991).
[11] K. Müller-Dethlefs, E. W. Schlag, E. R. Grant, K. Wang, and V. McKoy, Adv. Chem. Phys. **90**, 1 (1995).
[12] E. W. Schlag and R. D. Levine, Comments At. Mol. Phys. **33**, 159 (1997).
[13] I. I. Fabrikant, Zh. Eksp. Teor. Fiz. **79**, 2070 (1980) [Sov. Phys. JETP **52**, 1045 (1981)].
[14] V. D. Kondratovitch and V. N. Ostrovsky, Zh. Eksp. Teor. Fiz. **79**, 395 (1980) [Sov. Phys. JETP **52**, 198 (1980)]; J. Phys. B **17**, 1981 (1984); **17**, 2011 (1984); **23**, 21 (1990); **23**, 3785 (1990).
[15] C. Blondel, C. Delsart, and F. Dulieu, Phys. Rev. Lett. **77**, 3755 (1996).
[16] H. Helm, N. Bjerre, M. Dyer, D. Huestis, and M. Saeed, Phys. Rev. Lett. **70**, 3221 (1993).
[17] C. Bordas, M. J. Dyer, T. Fairfield, H. Helm, and K. C. Kulander, Phys. Rev. A **51**, 3726 (1995).
[18] C. Bordas, F. Paulig, H. Helm, and D. L. Huestis, Rev. Sci. Instrum. **67**, 2257 (1996).
[19] C. Bordas, M. J. Dyer, and H. Helm, J. Phys. IV **4**, C4-691 (1994).
[20] V. V. Beletzky, *Essays on the Motion of Celestial Bodies* (Mir, Moscow, 1977).
[21] F. Merkt and R. N. Zare, J. Chem. Phys. **101**, 3495 (1994).
[22] M. J. Vrakking and Y. T. Lee, J. Chem. Phys. **102**, 8818 (1995); **102**, 8833 (1995).
[23] M. J. Vrakking, I. Fischer, D. M. Villeneuve, and A. Stolow, J. Chem. Phys. **103**, 4538 (1995).